

MEASUREMENT AND CALCULATION OF CONTROL ROD WORTHS IN MASURCA

J.L. Kloosterman, Y. Rugama and M. Szieberth¹

Delft University of Technology, Interfaculty Reactor Institute,
Mekelweg 15, NL-2629 JB Delft, Netherlands

J.L.Kloosterman@iri.tudelft.nl

C. Destouches

(on behalf of the MASURCA team)

CEA/DEN/CAD, F-13108 Saint Paul-Lez-Durance, France

ABSTRACT

In this paper, an alternative derivation of the inverse point-kinetics equation is given based on the concept of micro-kinetics, which describes the fission rate in terms of prompt fission chains instead of single fission events. The concept is applicable to fast reactors with a short generation time and has been applied to measurements in the MASURCA reactor in Cadarache. In this reactor, two series of rod drop experiments have been conducted. Big discrepancies exist between the reactivity worth measured with different detectors, and spatial correction factors are needed to correct the measured count rates for the flux depression induced by the rods. These factors were calculated with the two-dimensional diffusion code FX2 applying an XY model of the reactor. The corrected control rod worth measured with monitor B differs significantly from the values measured with the other three monitors, and has been discarded from the analysis. The measured reactivity worth equals $11.7 \pm 0.2\%$ for rod BC1 and $13.5 \pm 0.4\%$ for rod BC2. The reactivity worth of BC1 calculated with MCNP is significantly lower ($10.8 \pm 0.2\%$), while the calculated value for BC2 agrees quite well within the margins of the experimental error ($13.2 \pm 0.2\%$). Surprisingly, there is quite a large difference for the reactivity worth of BC2 calculated with data from JEF-2.2 and ENDF/B-VI (13.6% and 12.9% , respectively). This needs further research. Taking into account the approximate solution method and geometrical models, the results from the XY diffusion calculations are in reasonable agreement with the Monte Carlo results (11.1% and 14.3% for rods BC1 and BC2, respectively).

1. INTRODUCTION

The MUSE project aims at a better understanding of the physics phenomena of sub critical reactors, with the ultimate aim to develop a reliable reactivity monitoring system for accelerator-driven systems. To this purpose the GENEPI deuterium accelerator has been placed adjacent to the MASURCA reactor in Cadarache, and a target (either deuterium or tritium) has been placed at the center of the reactor core. Many experiments are being conducted at this system, until now without the external neutron source in operation.

In this paper we describe some control rod drop experiments performed at MASURCA, and analyzed with inverse point-kinetics. Some interesting spatial effects were observed that obviously couldn't be explained by point kinetics and that needs a more sophisticated analysis. In section two of this paper, an alternative derivation of the inverse point-kinetics equations is given

¹ On leave from Budapest University of Technology and Economics, Institute of Nuclear Techniques, H-1111 Muegyetem rkp 9, Budapest

based on the concept of micro kinetics. Section three describes the experiments and shows the corresponding results from the inverse point kinetics analyses. Section four presents the calculations with 2-D diffusion and 3-D Monte Carlo codes to obtain the necessary data for the inverse point-kinetics analyses and the reactivity worth of the control rods. Section five presents the calculation results to obtain the spatial correction factors to the point kinetics analysis.

2. INVERSE POINT-KINETICS

The inverse point-kinetics method is a well-known method to determine the reactivity worth of the control rods in nuclear reactors. In fact, it is the most general method for measuring the so-called dynamic reactivity. The method is based on measuring the power of the reactor by neutron counters and solving the point-kinetics equations to calculate the dynamic reactivity $\rho(t)$. The starting point is the point-kinetics equations with one group of delayed neutrons:

$$\begin{aligned}\dot{n}(t) &= \frac{\rho(t) - \beta}{\Lambda} n(t) + \lambda c(t) + s(t) \\ \dot{c}(t) &= \frac{\beta}{\Lambda} n(t) - \lambda c(t)\end{aligned}\quad (2.1)$$

where $n(t)$, $c(t)$, and $s(t)$ are the time-dependent neutron density, precursor density and source density, respectively, β and λ are the delayed neutron fraction and the corresponding precursor decay constant, and Λ is the generation time. Solving these equations for the reactivity $\rho(t)$, one obtains [1,2]:

$$\rho(t) = \beta + \Lambda \frac{d}{dt} [\ln n(t)] - \lambda \beta \int_{-\infty}^t \frac{n(t')}{n(t)} \exp[-\lambda(t-t')] dt' - \Lambda \frac{s(t)}{n(t)} \quad (2.2)$$

In general, the kinetic parameters like Λ are difficult to calculate accurately, and should be known for all values of the reactivity (e.g. before and after the rod drop). Furthermore, often the source is not known, although methods exist to determine the source strength from the measurements [3]. For fast reactors with a very short generation time Λ , the above expression can be simplified considerably, as can be deduced from an alternative derivation of the inverse point-kinetics expression based on 'micro kinetics'.

In micro kinetics [4], one describes the neutron population in a reactor in terms of fission chains, which are initiated by either external source neutrons or decaying precursors. Except for the first neutron that induces the fission chain, all neutrons belonging to a fission chain are prompt ones. On the average, each fission chain starts with a fission neutron production rate of $\nu \Sigma_f = 1/\Lambda$ per second (prompt and delayed), or, equivalently, a precursor production rate of β/Λ per second, and decays exponentially with the prompt neutron decay constant $\alpha_p = (\rho(t) - \beta)/\Lambda$. In terms of micro-kinetics, a critical reactor is established when each fission chain produces exactly one precursor atom on the average.

Assuming a stationary fission chain density f_0 , the corresponding precursor density equals:

$$c_0 = \int_{-\infty}^t \int_{t'}^t f_0 \frac{\beta}{\Lambda} \exp\left[\frac{\rho_0 - \beta}{\Lambda}(t'' - t')\right] \exp[-\lambda(t - t'')] dt'' dt' = \frac{f_0 \beta}{\lambda(\beta - \rho_0)}, \quad (2.3)$$

which confirms that for a critical reactor with no source $\lambda c_0 = f_0$. For a sub-critical reactor with a constant fission chain density, one needs an external source with strength:

$$s_0 = \frac{-\rho_0}{\beta - \rho_0} f_0 \quad (2.4)$$

in order to have $\lambda c_0 + s_0 = f_0$. With constant reactivity, the neutron density is proportional to the fission chain density:

$$n_0 = \int_0^{\infty} f_0 \frac{1}{\Lambda} \exp\left[\frac{\rho_0 - \beta}{\Lambda} t\right] = \frac{f_0}{\beta - \rho_0}. \quad (2.5)$$

For a plutonium-fueled critical reactor ($\beta = 0.25\%$, $\rho_0 = 0$), the duration of an average fission chain is less than 150 generations, which, in case of MASURCA, takes less than 100 μs .

The expression for the reactivity (Eq. (2.2)) becomes very simple, if one may assume that the reactivity is constant during an average fission chain. Then the neutron density is always proportional to the fission chain density:

$$n(t) = \frac{f(t)}{\beta - \rho(t)} \quad (2.6)$$

where the reactivity is taken at the time instant where the fission chain is initiated. Assuming a constant precursor density c_0 for $t < 0$ and a constant source density s_0 at all time instants, the expression for the fission chain density for $t > 0$ becomes:

$$f(t) = \lambda c_0 \exp[-\lambda t] + \int_0^t \frac{\lambda \beta f(t')}{\beta - \rho(t')} \exp[-\lambda(t-t')] dt' + s_0 \quad (2.7)$$

When we divide all terms with $\beta - \rho(t)$, and substitute Eqs. (2.3), (2.4) and (2.5), we get for the neutron density:

$$n(t) = \frac{n_0 \beta}{\beta - \rho(t)} \exp[-\lambda t] + \frac{\lambda \beta}{\beta - \rho(t)} \int_0^t n(t') \exp[-\lambda(t-t')] dt' - \frac{\rho_0 n_0}{\beta - \rho(t)}, \quad (2.8)$$

from which the following expression for the reduced reactivity $\tilde{\rho}(t) = \rho(t)/\beta$ can be derived:

$$\tilde{\rho}(t) = \frac{1}{n(t)} \left[n(t) + n_0 (\tilde{\rho}_0 - \exp[-\lambda t]) - \lambda \int_0^t n(t') \exp[-\lambda(t-t')] dt' \right]. \quad (2.9)$$

Compared with Eq. (2.2) this expression has two advantages. First, it does not require the external source strength to be known (although the value of the initial reactivity $\tilde{\rho}_0$ is probably as hard to get as s_0), and secondly it makes no use of the generation time. The latter is a consequence of the fact that use is made of prompt fission chains, instead of individual fissions, which is only valid if the reactivity does not change during a prompt fission chain. For fast reactors, and certainly for MASURCA, this limitation poses no problem. As stated above, a prompt fission chain takes less than 100 μs , while a control rod drop that reduces the reactivity with about 10\$ takes more than one second. This means that the reactivity changes about 0.001\$ during a prompt fission chain, which indeed is negligible. For a sub-critical reactor, the duration of a fission chain is even shorter.

For six delayed neutron groups, Eq. (2.9) reads:

$$\tilde{\rho}(t) = \frac{1}{n(t)} \left[n(t) + n_0 \left(\tilde{\rho}_0 - \sum_{j=1}^6 \frac{\beta_j}{\beta} \exp[-\lambda_j t] \right) - \sum_{j=1}^6 \lambda_j \frac{\beta_j}{\beta} \int_0^t n(t') \exp[-\lambda_j(t-t')] dt' \right] \quad (2.10)$$

The integral at the RHS is evaluated recursively. If the value of the integral at time step t_n equals I_n its value at step t_{n+1} for delayed neutron group j is had from:

$$I_{n+1} = I_n \exp(-\lambda_j \Delta t) + \lambda_j \frac{\beta_j}{\beta} n(t_{n+1}) [1 - \exp(-\lambda_j \Delta t)] \quad (2.11)$$

with $\Delta t = t_{n+1} - t_n$.

3. MEASUREMENTS

Two series of measurements have been performed: one starting with the reactor in sub-critical state (June 2001) and four with the reactor in critical state (September 2001). Figures 3.1 and 3.2 show the layout of the core and the position of the fine-tuning rod BP and the control rods BC1 and BC2. In all experiments, first the fine-tuning rod BP had to be inserted, after which either BC1 or BC2 could be dropped.

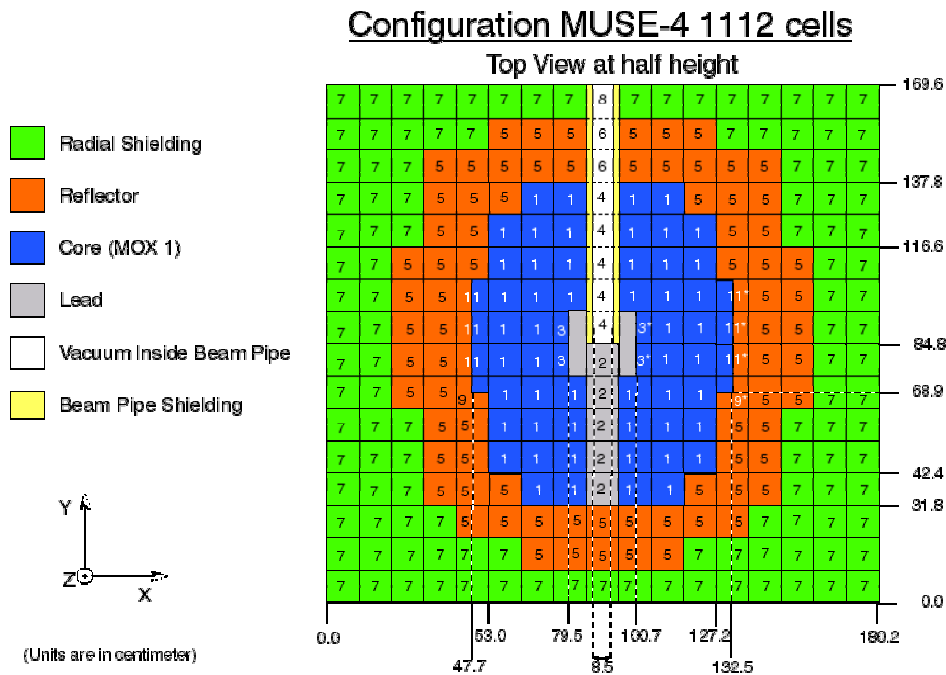


Figure 3.1: Layout of the MASURCA core.

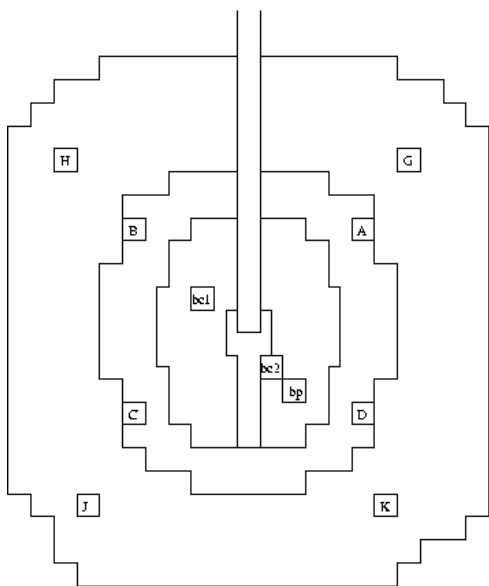


Figure 3.2: Position of the monitors A,B,C and D, and of the rods BP, BC1, and BC2.

In the June experiment the reactor was 0.537\$ sub critical when first the BP rod was dropped, secondly the BC2 rod, and thirdly the BC1 rod. In September four experiments were conducted: two in which the BC1 rod was dropped first, and two in which the BC2 rod was dropped first. It is noted that the core configuration changed meanwhile from subcritical to critical. Therefore, the results from the June measurement cannot be compared directly with those of September. From Eq. (2.10) can be seen that two input data are needed for the analysis: the initial reactivity $\tilde{\rho}_0$ and the delayed neutron data (λ_j, β_j) for six families. The calculation of the latter data is described in the next chapter. The initial reactivity $\tilde{\rho}_0$ can be derived from the experiments by the following procedure.

If the delayed neutron data is calculated for a specific state of the reactor, e.g. (virtual) critical, and if the reactor is held at that state for a certain period of time, the reactivity obtained from the inverse point-kinetics procedure should be constant for that same period too. This leaves one degree of freedom to fix the initial reactivity $\tilde{\rho}_0$. Because the delayed neutron data were calculated for a critical reactor (see next section), the initial reactivity is obtained by forcing the reactivity to a constant value before the rod drop.

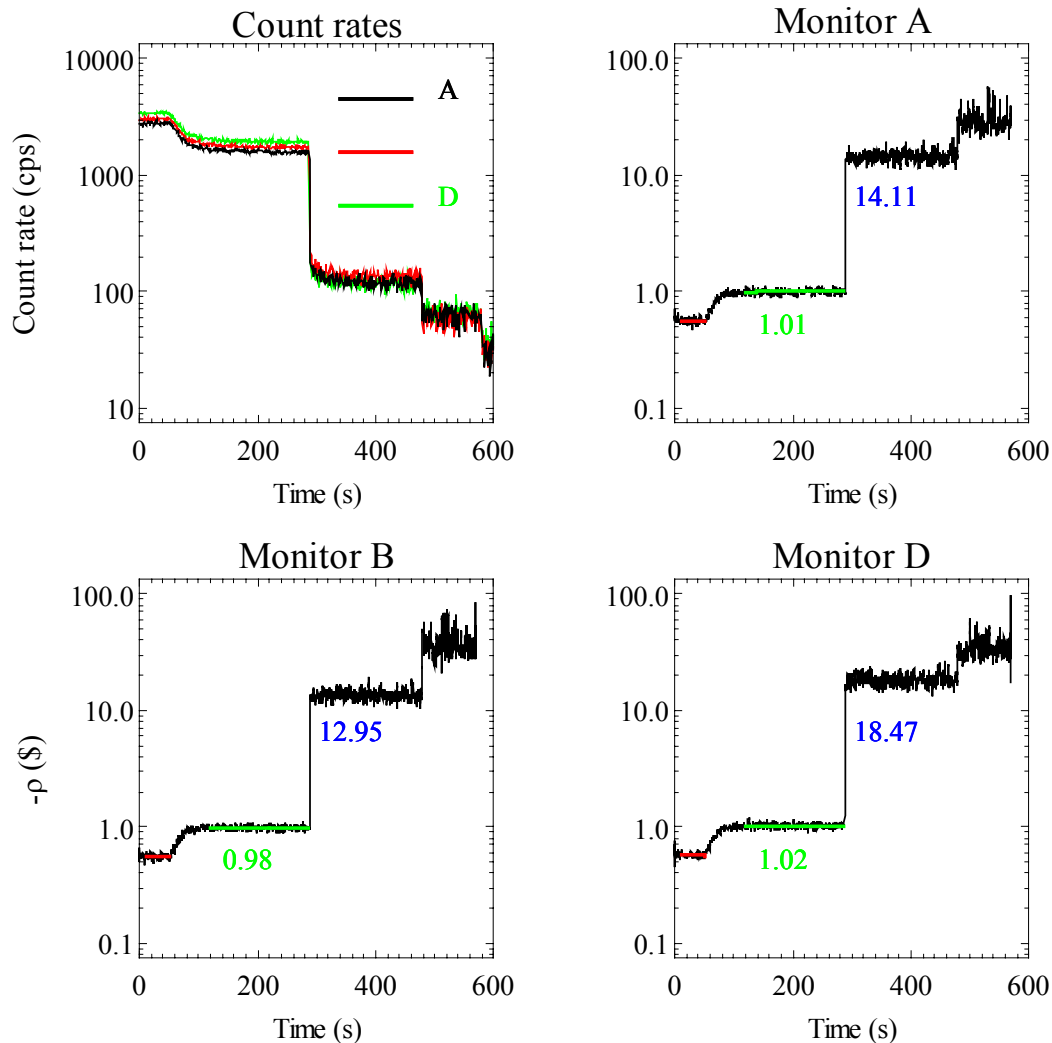


Figure 3.3: Count rates of monitors A, B, and D used in the June experiment and the corresponding reactivity values obtained by inverse point-kinetics. After about 50 s the BP rod was inserted, after 290 s the BC2 rod, and after 470 s the BC1 rod.

Figure 3.3 shows the count rates of the monitors A, B, and D and the corresponding reactivity as a function of time. The initial reactivity $\tilde{\rho}_0 = 0.565\$$ was (assumed to be) known. The reactivity value of the BC2 rod can be obtained by subtracting the reactivity at $t = 285$ s (obtained from a first-order polynomial fit for $120 < t < 285$ s) from the reactivity at $t = 295$ s (obtained from a first-order polynomial fit for $295 < t < 345$ s). The results are given in Table 4.2.

Similar results are given in Fig. 3.4 for one of the experiments performed in September starting with a critical reactor. The other measurement performed in September gives almost the same values (see Table 4.2), which indicates that the results can be reproduced quite accurately. In both Figs. 3.3 and 3.4, a large discrepancy can be seen for the reactivity of the BC2 rod as measured with different monitors. The same holds for the BC1 rod.

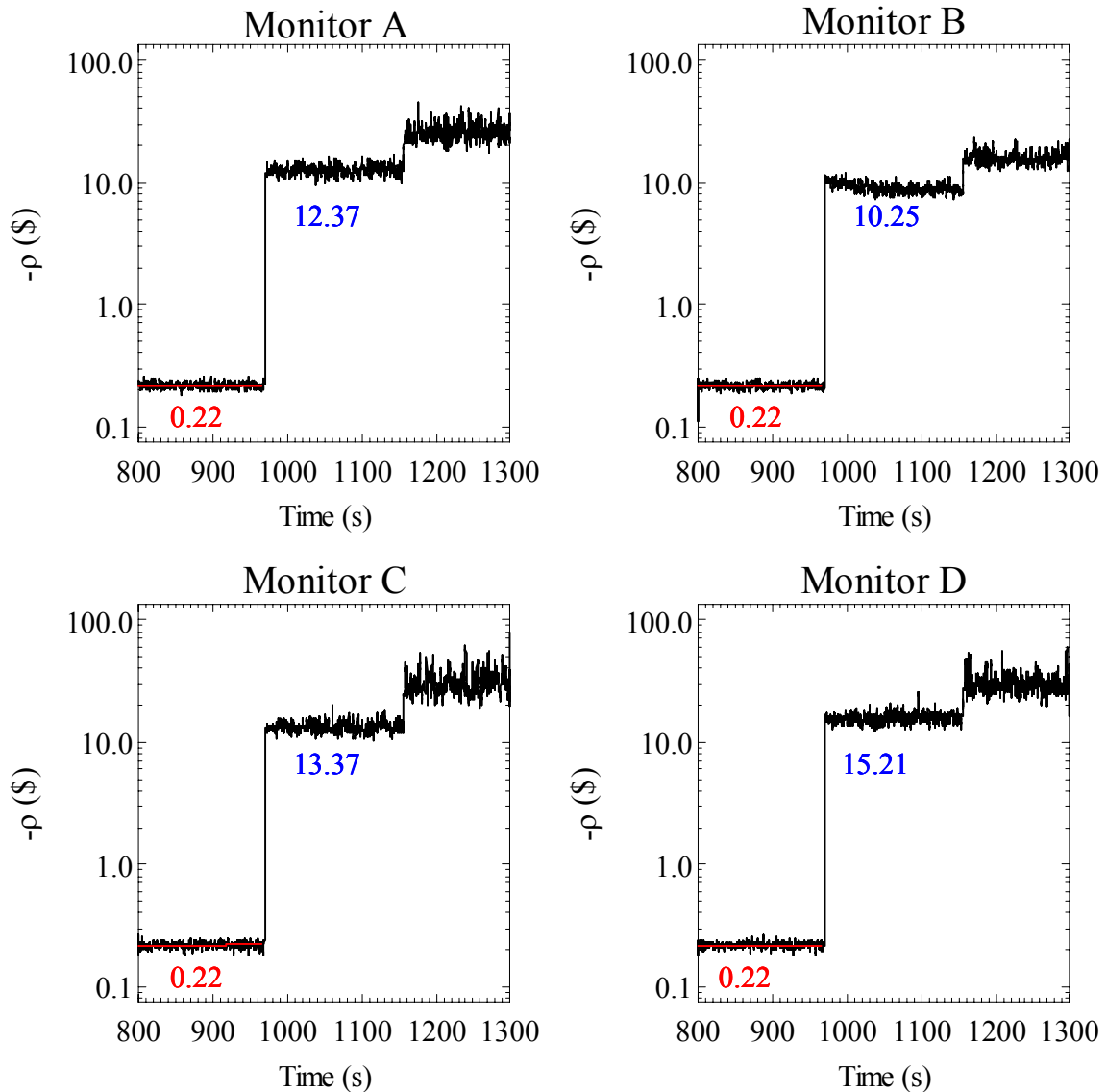


Figure 3.4: Reactivity values measured with monitors A, B, C and D used in one of the September experiments. Up to 960 s the reactor stabilizes after insertion of the BP rod. After 970 s the BC2 rod was dropped, and after 1150 s the BC1 rod. The initial reactivity was chosen such that the reactivity up to 950 is constant (slope $< 1E-5$ \$/s).

4. CALCULATIONS

4.1 CALCULATION OF DELAYED NEUTRON DATA

As mentioned before, the inverse point-kinetics method needs the delayed neutron data as input. The effective delayed neutron yields and the corresponding precursor decay constants for the six families were calculated by the FX2 diffusion code [5] using a 25-group cross section library prepared with the SCALE code system [6] and based on the JEF2.2 library [7]. The reactor model shown in Fig. 3.1 was converted to an RZ model with the lead target and the vacuum beam tube smeared. This approximation is expected to have only very mild influence on the effective (adjoint-weighted) delayed neutron fractions. The resulting one-group delayed neutron fraction (327 pcm) is in agreement with the data calculated by CEA. Table 4.1 gives the results of this calculation.

Table 4.1: The effective delayed neutron fraction and the corresponding precursor decay constants for six families calculated with FX2 using an RZ model of the MASURCA core.

λ_j (s^{-1})	1.324E-2	3.075E-2	1.236E-1	3.270E-1	1.187	3.459
β_j (pcm)	8.40	72.0	61.6	116.4	51.7	16.9

4.2 CALCULATION OF THE REACTIVITY WORTH WITH FX2

The above-mentioned two-dimensional diffusion code (FX2) and the 25-group nuclear data library were also used to calculate the reactivity worth of the control rods BC1 and BC2. To this end, the lead target and the vacuum beam tube in Fig. 3.1 were smeared, and three XY calculations were performed: one for the unrodded core, one for the BC1 rod inserted and one for the BC2 rod inserted. In all cases an axial buckling height of 50 cm was used to get a k_{eff} of nearly unity for the unrodded core. Fig. 4.1 gives the power profile for the unrodded core and for the BC2 rod fully inserted. The results for the reactivity worth of the rods are given in Table 4.2. In these calculations and in the MCNP calculations described in the next section, the BP rod was omitted, because its composition and that of the rod follower was not known accurately.

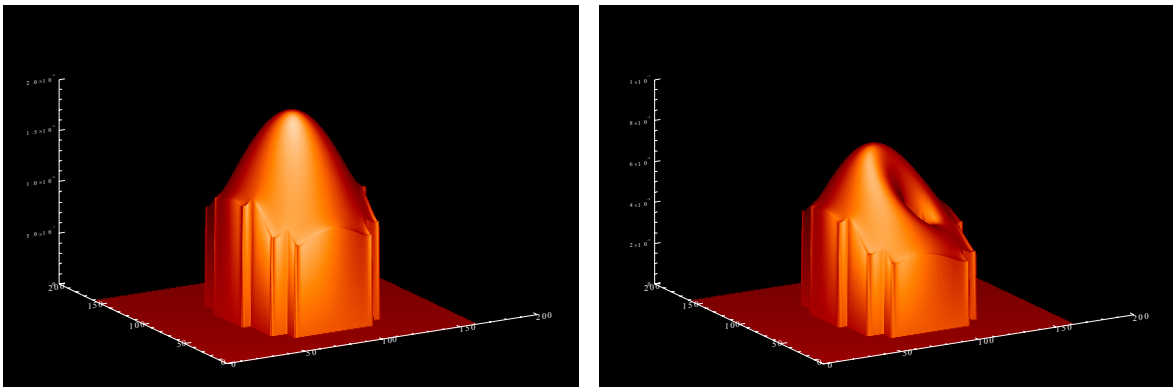


Fig. 4.1: The power profiles for the unrodded core (left) and for the core with the BC2 rod inserted.

4.3 CALCULATION OF THE REACTIVITY WORTH WITH MCNP

Of course, the above-mentioned calculations will be hampered with inaccuracies because of the approximate solution method and geometrical models. Therefore, accurate three-dimensional calculations were performed with the Monte-Carlo code MCNP [8] to get some kind of calculation reference solution. The results were performed both with nuclear data from the JEF2.2 and from the ENDF-B/VI nuclear data files. The results are given in Table 4.2.

Table 4.2: The reactivity worth measured and analyzed with inverse-point kinetics, compared with diffusion calculations (FX2) and Monte-Carlo calculations (MCNP). The statistical errors in the Monte Carlo calculations are less than 0.15\$.

$\bar{\rho}$ (\$)	June	Sept-I	Sept-II	FX2 JEF-2.2	MCNP JEF-2.2	MCNP ENDF-B/VI
BC1	A: B: D:	A: 10.6 B: 11.6 C: 11.2 D: 10.1	A: 10.7 B: 11.0 C: 11.2 D: 9.6	11.1	10.9	10.7
BC2	A: 13.1 B: 12.0 D: 17.4	A: 12.1 B: 10.0 C: 13.1 D: 15.0	A: 12.4 B: 9.9 C: 12.6 D: 14.7	14.3	13.6	12.9

5. SPATIAL CORRECTION FACTORS

As can be seen in Table 4.2, the difference between the reactivity worth measured with different monitors is quite large. This is due to the fact that the disturbance of the power profile (see Fig. 4.1) is such large that the inverse point-kinetics analysis is not valid anymore, especially for the monitors close to the control rods. Better values can be obtained when the influence of the spatial flux distribution on the count rates of the monitors is taken into account by spatial correction factors. The point-kinetic equations (Eqs. (2.1)) can be derived from the neutron transport equation by factorizing the neutron flux density $\phi(r, E, t)$ into a flux shape function $\psi(r, E, t)$ and an amplitude function $n(t)$:

$$\phi(r, E, t) = \psi(r, E, t)n(t). \quad (2.12)$$

One can shift the major part of the time dependence of the neutron flux density into the amplitude function by constraining the time dependence of the shape function [4]. To this end, a second equation is needed to hold some integral value of the shape function constant in time. Usually, the following constraint is chosen:

$$\iint_{V, E} \phi_0^*(r, E) \frac{\psi(r, E, t)}{v(E)} dEdV = K_0, \quad (2.13)$$

with $\phi_0^*(r, E)$ the adjoint function of the reference case (no rod inserted), and $v(E)$ the neutron velocity. The point-kinetics equations describe the behavior of the amplitude as a function of time, while the shape function describes the neutron flux as a function of space.

Of course, the shape factor changes when a control rod is inserted, and the count rate of a monitor should be adjusted to include this effect. Multiplying the count rate of a monitor after insertion of the control rod with the ratio of the shape functions before and after the rod drop can do this. Plotting this ratio for each position in the core gives the so-called correction surface, which is

shown for control rod BC2 in Fig. 5.1. The corrected reactivity worth of the control rods is given in Table 5.1, again together with the calculation values.

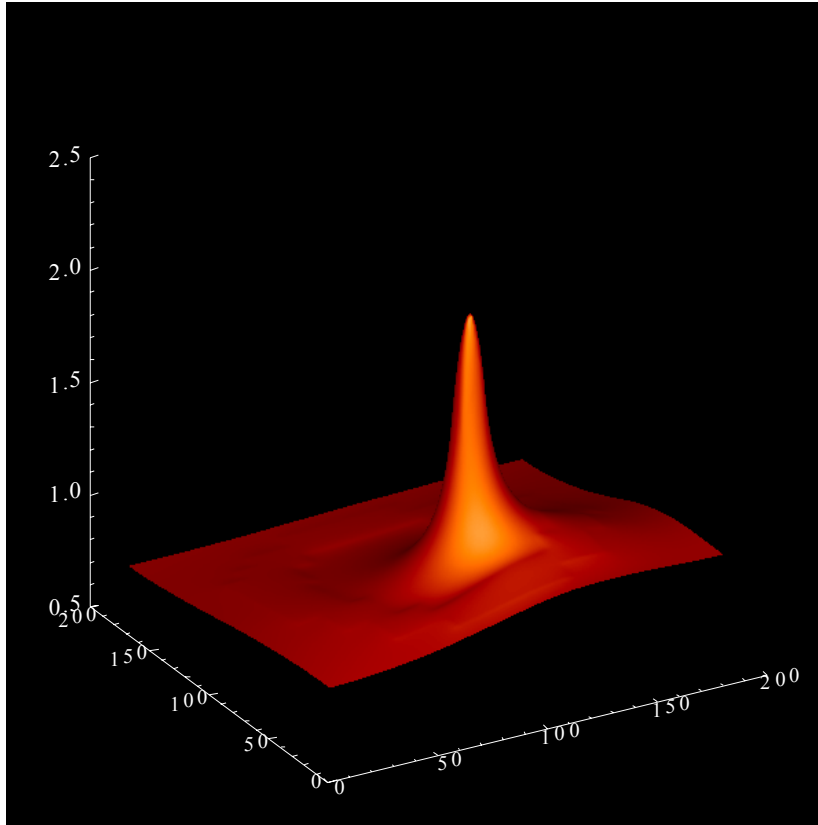


Figure 5.1 Correction surface for the insertion of the control rod BC2. At the position of the rod BC2 the correction surface reaches a value of 1.8, while at the periphery it is about 0.8.

Table 5.1: The reactivity worth measured and analyzed with inverse-point kinetics and **corrected** for the change of the spatial shape function, compared with diffusion calculations (FX2) and Monte-Carlo calculations (MCNP). Only the measured values differ from Table 4.2. The statistical errors in the Monte Carlo calculations are less than 0.15\$.

$\bar{\rho}$ (\$)	June	Sept-I	Sept-II	FX2 JEF-2.2	MCNP JEF-2.2	MCNP ENDF-B/VI
BC1	A: - B: - C: - D: -	A: 11.6 B: 9.3 C: 11.7 D: 11.9	A: 11.8 B: 8.9 C: 11.6 D: 11.4	11.1	10.9	10.7
Average		11.7±0.2*			10.8	
BC2	A: 14.9 B: 14.5 C: - D: 15.3	A: 13.7 B: 12.0 C: 14.0 D: 13.2	A: 13.9 B: 11.8 C: 13.4 D: 13.0	14.3	13.6	12.9
Average	14.9±0.5	13.5±0.4*			13.2	

*Averaged over the results of monitors A, C, and D. Results of monitor B have been discarded.

6. DISCUSSION AND CONCLUSIONS

For fast reactors the inverse point-kinetics equations can be simplified by applying the concept of prompt fission chains, which "lump" all fission events that are induced by the same initial source neutron. Applying this concept, one does not need the generation time, although one has to be sure that its value is sufficiently small. Rod drop experiments in MASURCA have shown that the inverse point-kinetics analysis is not sufficiently accurate. Spatial effects that can obviously not be accounted for in point kinetics need corrections that can be obtained from calculation analysis. The reactivity worth of the rod BC2 during the June experiments (sub critical reactor) deviates from the experiments at critical. Apparently the core configuration has been modified so strongly that this significantly influences the control rod worth.

In the September measurements, the control rod worth measured with monitor B is significantly lower than the other values. Because, this monitor has shown before to be unstable, it has been discarded from further analyses. Monitors A, C, and D do give coherent results for the reactivity worth of both rods. The reactivity worth averaged over these results are $11.7 \pm 0.2\%$ for BC1 and $13.5 \pm 0.4\%$ for BC2.

The reactivity worth of BC1 calculated with MCNP is significantly lower ($10.8 \pm 0.2\%$), while the calculated value for BC2 ($13.2 \pm 0.2\%$) agrees quite well within the margins of the experimental error. Surprisingly, there is quite a large difference for the reactivity worth of BC2 calculated with data from JEF-2.2 and ENDF/B-VI (13.6% and 12.9% , respectively). Because this is not seen for the BC1 rod, this discrepancy might be caused by the nuclear data of the lead target. This needs further research Taking into account the approximate solution method and geometrical models, the results obtained from the two-dimensional diffusion calculations are in reasonable agreement with the Monte Carlo results.

ACKNOWLEDGEMENTS

The authors acknowledge the European Commission for co-funding this work under project number FIKW-CT2000-00063, and the other members of the MUSE team for their cooperation.

REFERENCES

1. J. J. Duderstadt and L. J. Hamilton, *Nuclear Reactor Analysis*, John Wiley&Sons, Inc., (1976)
2. M. Ash, *Nuclear Reactor Kinetics*, McGraw-Hill, Inc., (1979)
3. J. E. Hoogenboom and A. R. van der Sluijs, "Neutron Source Strength Determination for On-Line Reactivity Measurement", *Annals of Nuclear Energy*, **15**, pp.553-559 (1988).
4. Karl O. Ott and Robert J. Neuhold, *Introductory Nuclear Reactor Dynamics*, American Nuclear Society, (1985)
5. R. A. Shober, T. A. Daly, and D. R. Ferguson, "FX2-TH: A Two-Dimensional Nuclear Reactor Kinetics Code with Thermal-Hydraulic Feedback", Argonne, Illinois 60439, (1978).
6. "SCALE 4.2, Modular Code System for Performing Standardized Computer Analyses for Licensing Evaluations", Oak Ridge, Tennessee, (1994).
7. "The JEF-2.2 Nuclear Data Library", Nuclear Energy Agency, Paris, (2000).
8. J. F. Briesmeister, "MCNP-4C General Monte Carlo N-Particle Transport Code", Los Alamos, LA-13709-M, (2000).